Published in final edited form as:
Chem Commun (Camb). 2012 April 7; 48(28): 3385–3387. doi:10.1039/c2cc17852d.

Synthesis of β-cyclodextrin conjugated superparamagnetic iron oxide nanoparticles for selective binding and detection of cholesterol crystals†

Hongguang Li[‡,a], **Mohammad H. El-Dakdouki**[‡,a], **David C. Zhu**[b,c], **George S. Abela**[d], and **Xuefei Huang**[*,a,c]

[a]Department of Chemistry, Michigan State University, East Lansing, Michigan, 48824, USA

[b]Departments of Radiology and Psychology, Michigan State University, East Lansing, Michigan, 48824, USA

[c]Biomedical Imaging Research Centre, Michigan State University, East Lansing, Michigan, 48824, USA

[d]Department of Medicine, Division of Cardiology, Michigan State University, East Lansing, Michigan, 48824, USA

Abstract

Water-soluble, β-cyclodextrin conjugated superparamagnetic nanoparticles have been constructed. These particles showed selective binding to cholesterol crystals, which opens the door for the detection of cholesterol crystal-related diseases such as atherosclerosis by magnetic resonance imaging (MRI).

Cardiovascular disease, which is often associated with atherosclerosis, is the leading cause of death and disability in the world, and its prevalence and economic burden are expected to continue to rise. Atherosclerotic plaques are formed through the accumulation of large amounts of cholesterol, cellular debris, macrophages, and fibrous connective tissue underneath the endothelium lining in artery walls.[1] The high local concentration of cholesterol leads to the formation of cholesterol crystals in the plaques. Studies have revealed that cholesterol crystals accumulated in the plaques can puncture through the fibrous tissues capping the plaques.[2-5] This process weakens the fibrous cap and can cause plaque rupture leading to heart attacks and strokes. Furthermore, recent research has shown that cholesterol crystals can induce inflammation in plaques by themselves,[6] which further destabilizes the plaques. Thus the development of a method to detect the presence of cholesterol crystals can provide a new approach to evaluate the risk of acute cardiac events. Herein, we report our results obtained by using a magnetic nanoparticle (MNP) based system to selectively bind and detect cholesterol crystals by MRI.

As a non-invasive method, MRI is a widely-used approach to image a variety of human diseases. However, MRI alone often cannot give sufficient contrasts to enable target detection. In recent years, due to their high relaxivity and biocompatibility, superparamagnetic iron oxide nanoparticles (SPIONs) have emerged as an attractive agent to

†Electronic supplementary information (ESI) available: Experimental details, TEM, TGA, UV-vis measurements. See DOI: 10.1039/c2cc17852d

*xuefei@chemistry.msu.edu; Fax: +1-517-353-1793; Tel: +1-517-355-9715 ext 329 .
‡These authors contributed equally to this work.

enhance the image contrast in MRI.[7-9] To detect cholesterol crystals using SPIONs, the key requirement is the grafting of specific ligands onto nanoparticle (NP) surface to recognize cholesterol crystals.

Although several antibodies and proteins are known to bind cholesterol either in its soluble form or as crystals,[10-12] they are expensive, prone to denaturation and can be immunogenic. These considerations prompted us to explore small molecule targeting agents. β-Cyclodextrin (β-CD) is a cyclic molecule formed by seven α-1,4 linked D-glucopyranoside units. Cholesterol dissolved in water can enter the hydrophobic interior of β-CD, forming a host-guest inclusion complex with two β-CD molecules.[13,14] However, it is unknown whether β-CD is capable of binding cholesterol crystals. We envision that some cholesterol molecules should partially protrude out from the surface of the crystals, which should enable their binding by β-CD. With many copies of β-CD on the exterior, the β-CD MNPs should be able to simultaneously interact with multiple cholesterols, which can lead to high affinity binding with the crystal leading to contrast changes in MRI.

To test this possibility, we began by immobilizing β-CD onto MNPs (Scheme 1). The MNP SPIONs were synthesized through a coprecipitation method by heating a 2: 1 molar ratio of ferric chloride and ferrous chloride in the presence of dextran and ammonium hydroxide.[15,16] This was followed by the treatment with epichlorohydrin to crosslink the dextran coating producing NP **1**, which was aminated with ammonium hydroxide. In order to conjugate β-CD onto MNPs, commercially available carboxymethyl-β-CD was utilized, which has on average three carboxymethyl groups per β-CD. The amide bond formation between NH_2-NP **1** and carboxymethyl-β-CD was mediated by 2-chloro-4,6-dimethoxy-1,3,5-triazine (CDMT), with residual amine groups capped with methoxy acetic acid to reduce potential non-specific interactions. NP **1** and NP **2** were thoroughly characterized by transmission electron microscopy (TEM), powder X-ray diffraction (XRD), thermogravimetric analysis (TGA), dynamic light scattering (DLS), zeta potential, magnetic moment measurement, infrared and UV-vis spectroscopy (see ESI†). On average, there were 125 β-CD molecules on each NP (Fig. S2, ESI†). NP **2** is superparamagnetic as evident from the absence of a hysteresis loop measured by a superconducting quantum interference devices (SQUID) magnetometer (Fig. S4, ESI†).

To determine whether NP **2** can bind cholesterol crystals, an enzyme-linked immunosorbent assay (ELISA) was established. Cholesterol crystals were deposited into the wells of an ELISA plate. NPs of increasing concentrations were incubatedwith the crystals in the plate. Upon washing off the unbound NPs, a plant lectin concanavalin A (ConA) conjugated with horseradish peroxidase (HRP) was added to the wells. ConA is known to recognize glucopyranoside,[17] thus is able to bind with the dextran coating on the NP surface. The HRP conjugated to ConA can catalyze the conversion of a chromogenic substrate 3,3′,5,5′-tetramethylbenzidine (TMB) into yellow colored molecules upon addition of sulfuric acid. The relative amounts of NPs bound to the cholesterol crystals on the plate could then be determined by measuring the optical density (OD) at 450 nm. As shown in Fig. 1, the β-CD coated NP **2** exhibited a dose dependent binding to cholesterol crystals with 50% binding achieved at a NP concentration of 0.05 mg mL^{-1}. NP binding to cholesterol crystals was significantly reduced when free β-CD (15 mg mL^{-1}) was added together with NP **2** during incubation presumably due to the competitive binding of free β-CD to the crystals. The large amount of free β-CD required for competitive binding highlighted the high avidity of NP **2** with the crystal due to the polyvalency effect.[18] As a control, SPION or NP **1** without β-CD exhibited minimal retention on the ELISA plate even at a NP concentration of 0.4 mg mL^{-1}.

†Electronic supplementary information (ESI) available: Experimental details, TEM, TGA, UV-vis measurements. See DOI: 10.1039/c2cc17852d

These results suggest that the binding between NP **2** and cholesterol crystals mainly originates from the molecular recognition between the grafted β-CD and cholesterol crystals.

To confirm the binding between NP **2** and cholesterol crystals, a variety of other techniques were used. Upon incubation of an aqueous solution of NP **2** (0.8 mg mL^{-1}, 1 mL) with cholesterol crystals (2 mg), the white crystals became brown, indicating the adsorption of NP **2** onto the crystal surface. Treatment of the crystals with Prussian blue, a staining method specific for the detection of ferric ion, generated a striking blue color on the crystal (Fig. 2a and c). In contrast, crystals incubated with NP **1** of the same concentration were only lightly blue (Fig. 2a and b), implying minimal adsorption of NP **1** onto cholesterol crystals.

As our long term goal is to non-invasively detect the cholesterol crystals in vivo, we tested the possibility of imaging NP **2** bound crystals by MRI. The MNPs were found to have high T2* relaxivity (Rr2* = 122 mM^{-1} s^{-1} for MNP 2) (Fig. S5, ESI†), suggesting that they are good contrast agents for T2* weighted imaging. Cholesterol crystals incubated with NP **1** and NP **2**, respectively, were embedded in a polyacrylamide gel matrix and subjected to MRI using a 3D Fast SPoiled Gradient Recalled (FSPGR) sequence. The T2* weighted images of cholesterol crystals incubated with NP **1** exhibited no significant difference from the background, suggesting that there was little retention of NP **1** on crystals and crystals alone could not produce sufficient contrast from their environment for MRI detection. In comparison, the T2* weighted images clearly showed dark spots with NP **2** treated crystals due to the magnetic field inhomogeneity caused by the presence of the superparamagnetic NPs (Fig. 2d). These results corroborated the Prussian blue staining images and highlighted the need for targeting contrast agents.

To enable the direct observation of NPs binding to cholesterol crystals, a fluorescent probe, fluorescein isothiocyanate (FITC), was conjugated to NP **2** (FITC-NP **2**, Scheme 1). The successful FITC conjugation was proven by UV-vis measurements, which revealed a characteristic absorption peak of fluorescein around 496 nm from FITC-NP **2** (Fig. S6, ESI†). After incubation with cholesterol crystals, the binding of FITC-NP **2** was clearly observed by confocal fluorescence microscopy where the adsorbed FITC-NP **2** showed a green color on the crystal (Fig. 2g and h). In comparison, cholesterol crystals treated with the FITC labeled NP **1** only exhibited weak green fluorescence (Fig. 2e and f) further supporting the important role that β-CD plays in crystal binding.

In order to mimic *in vivo* conditions and test the selectivity of NP **2** in a biological system, cross sections of rabbit aorta tissue (50 μm thick slices) were immobilized on glass slides. A cholesterol solution in ethanol was carefully deposited on half of the tissue on the slide. Upon evaporation of ethanol, crystals were formed only in half of the tissue with the other half serving as a control since the two halves have similar morphology and molecular compositions. Incubation of the whole tissue with NP **2** followed by Prussian blue staining exhibited striking difference in staining levels, with the cholesterolladen half of the tissues yielding much stronger Prussian blue stain (Fig. S7, ESI†). Importantly, NP **1** lacking β-CD coating did not bind strongly to the tissues with or without cholesterol crystal deposits.

In another experiment, sections of atherosclerotic rabbit aorta tissues were incubated with both NP **1** and **2** without exogenous cholesterol crystal deposition. As discussed above, in atherosclerotic plaques, there are large quantities of cholesterol crystals.[2-5] Prussian blue staining of the tissues after NP **2** incubation showed the accumulation of NPs and strong blue color in plaque areas (Fig. 3a). In comparison, NP **1** gave only weak Prussian blue staining of the tissue. This was further confirmed by TEM studies. NPs were clearly

observed in tissues incubated with NP **2** in TEM images (Fig. 3c) as supported by X-ray photoelectron spectroscopy (Fig. S8b, ESI†), while few NPs were present in tissues incubated with NP **1** (Fig. 3b and Fig. S8a, ESI†). Together, these results suggest that in a complex biological environment such as a tissue, NP **2** displayed good selectivity towards cholesterol crystal binding and the binding was β-CD dependent.

In conclusion, we have fabricated new β-CD coated MNPs, which showed selective binding to cholesterol crystals both *in vitro* and *ex vivo*. To the best of our knowledge, this is the first time that such a system became available for molecular imaging of cholesterol crystals. By taking advantage of the superparamagnetic properties of the iron oxide core and the molecular recognition between β-CD and cholesterol, these β-CD coated MNPs can be promising candidates for the non-invasive detection of the crystalized cholesterol in atherosclerotic plaques *in vivo* by MRI.

Supplementary Material

Refer to Web version on PubMed Central for supplementary material.

Acknowledgments

This work was partially supported by an NSF CAREER award and the National Cancer Institute (R01-CA149451) (XH). We would like to thank the Department of Radiology, Michigan State University, for their very generous support towards access of the MRI scanner.

References

1. Sanz J, Fayad ZA. Nature. 2008; 451:953–957. [PubMed: 18288186]
2. Abela GS, Aziz K. Clin. Cardiol. 2005; 28:413–420. [PubMed: 16250264]
3. Abela GS, Aziz K. Scanning. 2006; 28:1–10. [PubMed: 16502619]
4. Vedre A, Pathak DR, Crimp M, Lum C, Koochesfahani M, Abela GS. Atherosclerosis. 2009; 203:89–96. [PubMed: 18703195]
5. Abela GS, Aziz K, Vedre A, Pathak D, Talbott JD, DeJong J. Am. J. Cardiol. 2009; 103:959–968. [PubMed: 19327423]
6. Duewell P, Kono H, Bauernfeind F, Sirois CM, Rock KL, Abela GS, Nunez S, Espevik T, Moore K, Fitzgerald K, Wright SD, Hornung V, Latz E. Nature. 2010; 464:1357–1361. [PubMed: 20428172]
7. Neuwelt EA, Hamilton BE, Varallyay CG, Rooney WR, Edelman RD, Jacobs PM, Watnick SG. Kidney Int. 2009; 75:465–474. [PubMed: 18843256]
8. Thorek DLJ, Chen AK, Czupryna J, Tsourkas A. Ann. Biomed. Eng. 2006; 34:23–38. [PubMed: 16496086]
9. Bulte JWM, Kraitchman DL. NMR Biomed. 2004; 17:484–499. [PubMed: 15526347]
10. Lammert F, Sudfeld S, Busch N, Matern S. World J. Gastroenterol. 2001; 7:198–202. [PubMed: 11819760]
11. Perl-Treves D, Kessler N, Izhaky D, Addadi L. Chem. Biol. 1996; 3:567–577. [PubMed: 8807889]
12. Swartz GM, Gentry MK, Amende LM, Blanchettemackie EJ, Alving CR. Proc. Natl. Acad. Sci. U. S. A. 1988; 85:1902–1906. [PubMed: 3162316]
13. Asanuma H, Kakazu R, Shibata M, Hishiya T, Komiyama M. Supramol. Sci. 1998; 5:417–421.
14. Breslow R, Zhang BL. J. Am. Chem. Soc. 1996; 118:8495–8496.
15. Palmacci, S.; Josephson, L.; Groman, EV. Synthesis of Polysaccharide Covered Superparamagnetic Oxide Colloids. US Patent WO/1995/005669. 1995.
16. Kamat M, El-Boubbou K, Zhu DC, Lansdell T, Lu XW, Li W, Huang X. Bioconjugate Chem. 2010; 21:2128–2135.
17. Shimura K, Kasai K. Anal. Biochem. 1995; 227:186–194. [PubMed: 7668380]
18. Mammen M, Choi S-K, Whitesides GM. Angew. Chem., Int. Ed. 1998; 37:2754–2794.

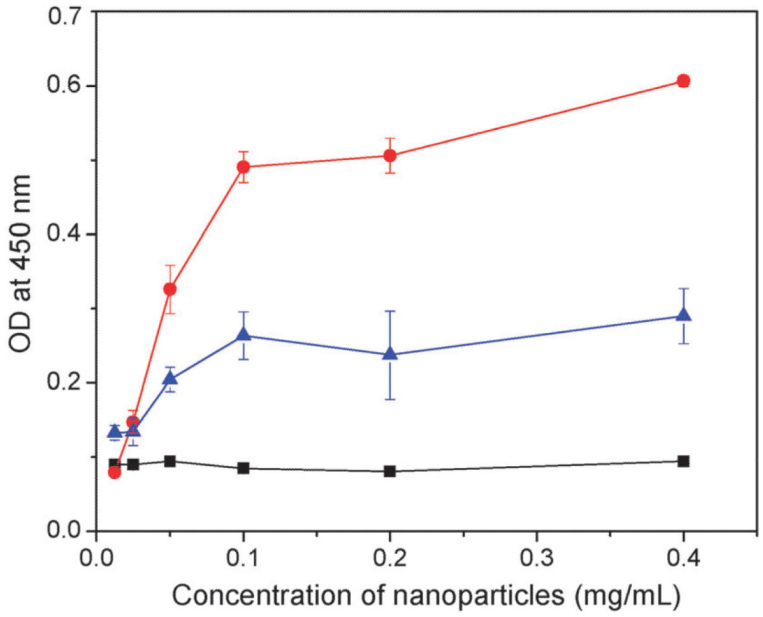

Fig. 1.

Binding between NP **2** and cholesterol crystals in the absence (red circles) and presence (blue triangles) of free β-CD (15 mg mL^{-1}) as determined by ELISA. As a control, NP **1** and SPION did not show any binding to cholesterol crystals. For clarity, only the ELISA results of NP **1** and cholesterol crystal binding (black squares) are shown. The amount of cholesterol crystals deposited in each well is 0.2 mg.

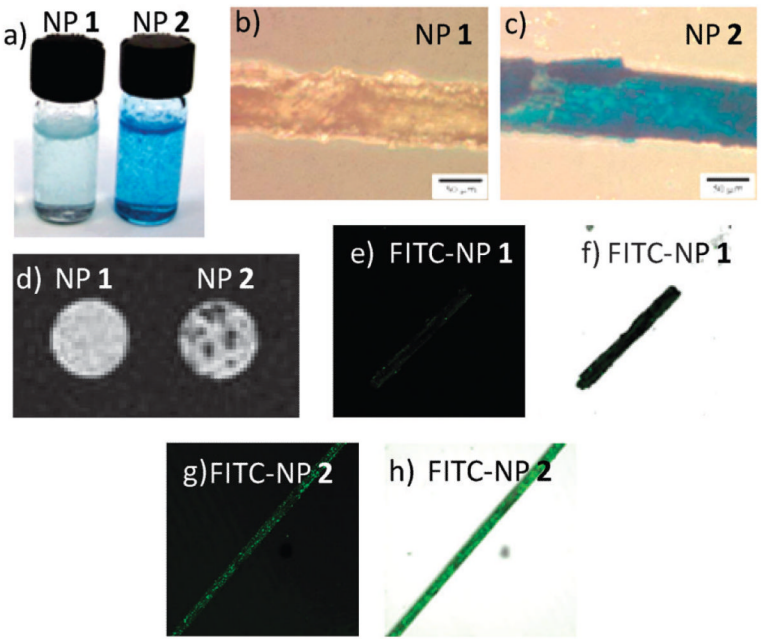

Fig. 2.

(a) Cholesterol crystals (2 mg) incubated with aqueous solutions of NP **1** (left) and NP **2** (right), and then treated with Prussian blue stain. The concentrations of nanoparticles were 0.8 mg mL^{-1} and incubation was carried out at 37 °C for 16 hours. (b) The cholesterol crystal/NP **1** complex and (c) the cholesterol crystal/NP **2** complex on a glass slide after Prussian blue staining. The scale bar is 50 μm. (d) T2* weighted MRI images of the cholesterol crystals after incubation with NP **1** (left) and NP **2** (right). Confocal microscopy images of cholesterol crystals after incubation with NP **1** and NP **2**. (e) FITC channel and (f) overlay of the laser image with FITC channel of FITC-NP **1**/cholesterol; (g) FITC channel and (h) overlay of the laser image with FITC channel of FITC-NP **2**/cholesterol.

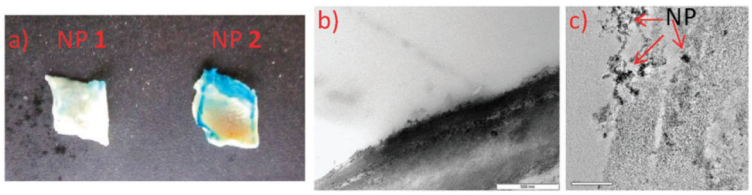

Fig. 3.

(a) Light microscopy images of rabbit atherosclerotic aorta tissues (~1 cm) incubated with an aqueous solution (0.78 mg mL^{-1}) of NP **1** and NP **2** for 24 hours followed by Prussion blue staining. The plaques were found along the edges of these tissues. TEM images of (b) NP **1** and (c) NP **2** incubated with the atherosclerotic aorta tissues.

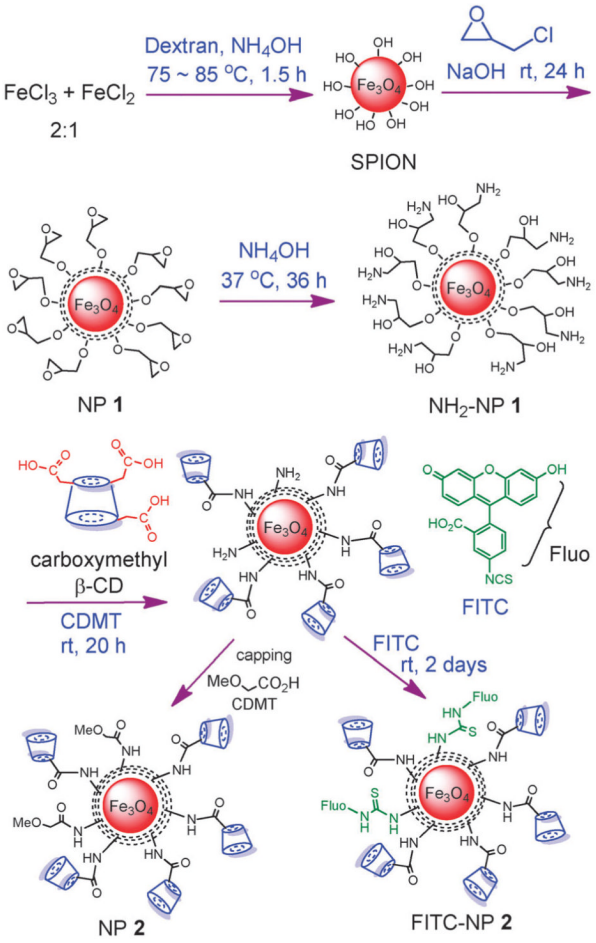

Scheme 1.

Preparation of β-CD conjugated MNPs. The functional group transformation in each step is shown. The MNP core and coatings are not drawn to scale.